

THERMOPLASTIC MODELING OF UNDRAINED FAILURE OF SATURATED CLAY DUE TO HEATING

TOMASZ HUECKEL¹⁾ and RITA PELLEGRINI¹⁾

ABSTRACT

This paper is concerned with modeling of thermomechanical failure of triaxial specimens of saturated clays of low porosity. Thermomechanical failure manifests itself in undrained conditions as a development of advanced irreversible strains due to heating under constant total stress. In experiments on two clays the failure occurred at temperatures from 70° to 90°C. The observed failure is associated with a pore water pressure buildup. Models of thermoplastic behavior of skeleton and of thermal volume changes of adsorbed water are employed to interpret and numerically simulate the test results. Using these models, thermomechanical failure was found to occur when the effective stress is brought to the critical state by expansion of pore water and thermoplastic compressive strain in skeleton.

Key words: clay, failure, thermoplasticity, undrained heating (IGC: D6/D8/E13)

INTRODUCTION

This paper deals with modeling of thermomechanical failure of saturated clays and silty clays tested at high stresses in triaxial undrained conditions. The term thermomechanical failure is introduced to describe relatively large, irreversible, compressive, axial strains that develop in clay specimens in response to heating. Laboratory experiments show that thermomechanical failure may occur at temperatures as low as 70°C and at a constant total stress state considered as "safe", i. e., close to the state of stress in situ.

The detrimental effect of temperature raise

on the behavior of the seabed and continental clays as well as the clay based buffers in hard rocks may become important in nuclear waste isolation (Davies and Banerjee, 1980; Hueckel and Peano, 1987; Pusch, 1987). Clay failure may increase permeability and enhance the migration of radionuclides in the presence of groundwater flow. Also, when associated with a hydraulic fracturing or formation of dilatant zones this may decrease thermal conductivity of clays by formation of water filled pockets (Tassoni, 1980). Thermomechanical failure has been discussed by Davies and Banerjee (1980). It was also observed in oil sands by Agar et al. (1986), who gave an exhaustive

¹⁾ Associate Professor, Department of Civil and Environmental Engineering, Duke University, Durham, NC 27706, USA.

¹⁾ Senior Engineer, ISMES, Bergamo, ITALY.

Manuscript was received for review on March 6, 1990.

Written discussions on this paper should be submitted before April 1, 1992, to the Japanese Society of Soil Mechanics and Foundation Engineering, Sugayama Bldg. 4 F, Kanda Awaji-cho 2-23, Chiyoda-ku, Tokyo 101, Japan. Upon request the closing date may be extended one month.

phenomenological interpretation to this effect.

In terms of total stress the above described behavior of clay may be seen as a heat induced creep. However, the pore water pressure buildup measured during heating indicates that thermomechanical failure in undrained conditions may result from differential thermal strain in skeleton and in clay water. The objective of this paper is to attempt to explain the observed behavior in terms of a model of non-viscous, irreversible response of the skeleton and of non-linear thermoelastic response of adsorbed water. The validity of generalized Terzaghi's effective stress principle is accepted.

The response of skeleton and of adsorbed water is modeled separately. First, it is assumed that thermal strain in the skeleton may be determined from tests in drained conditions. The pioneering study by Campanella and Mitchell (1968) indicated that in drained conditions high porosity clays reveal a complex pattern of volume changes due to heating. At low porosity, overconsolidated and normally consolidated clays behave differently (Hueckel and Peano, 1987; Hueckel and Baldi, 1990). In overconsolidated clays, thermally induced volumetric strains are either expansive or contractile, and predominantly reversible, depending on the effective stress and temperature applied. In normally consolidated clays, the volumetric strains are much larger, predominantly irreversible, and contractile. Since the work of Campanella and Mitchell (1968), it is believed that contractile thermal volumetric strains in clays are related to the behavior of the water that is adsorbed around clay particles. Pusch (1987) and Pusch and Guven (1987) observed irreversible microstructural changes in a Na bentonite saturated clay at 150–300°C. The stacks of montmorillonite flakes showed a denser grouping, the voids between the stacks became larger than in the unheated material, and the collapse of interlamellar voids occurred.

Irreversible and reversible thermal strains in skeleton as resulting from drained tests may be described by employing concepts of thermo-plasticity theory (Prager, 1958). This theory

has been used to adapt the modified Cam-clay model (Roscoe and Burland, 1968) to thermal loading (Hueckel et al., 1987 a and b; Hueckel and Borsetto, 1990).

Thermal volume change in pore water results from its thermal expansion and possible release of the interlamellar water (Dierjaguin et al., 1987; Claesson et al., 1986; Pusch and Guven, 1988). In low porosity clays, a water thermal volumetric strain appears to be smaller than the thermal expansion of bulk water (Baldi et al., 1988). This may be attributed to several electrochemical and chemical micro-mechanisms in clay pore spaces (Derjaguin et al., 1987; Low, 1987). A semi-empirical formula for thermal volume change in clay water was proposed by Baldi et al. (1988).

In this paper the above mentioned models for skeleton thermoplasticity and thermal volume change for pore water are combined, in an attempt to analyse numerically thermomechanical failure due to undrained heating. The models are briefly described in Section 2, while relative equations are to be found in Appendices A and B. The experiments are described in Section 3. In Section 4 two possible variants of failure development are discussed, in which the skeleton response to heating is either initially elastic and then plastic or plastic from the very beginning. Plastic strain hardening and strain softening are discussed in relation to thermal softening. In Section 5 water pressure buildup to failure and temperature to failure are numerically determined and compared to experimental values.

OUTLINE OF A THERMOPLASTIC MODEL FOR SATURATED CLAYS

The model which will be employed is described in a general form elsewhere (Hueckel et al., 1987a and 1987b; Hueckel and Borsetto, 1990). It is based on Prager's thermo-plasticity theory (Prager, 1958) and on modified Cam-clay model (Schofield and Wroth, 1968; Burland and Roscoe, 1968). Here, it is combined with a model for thermoelastic expansion of interstitial water in low porosity clays, (Baldi et al., 1988).



Fig. 1.
to t

The f
behavior
the expe
(Huecke
Baldi, 19

The s
within t
elastic, a
at the yie
surface in
of plastic
(strain h
depending
metric s
negative(
modified
1968). In
elastic d
temperatu
occurs, F
as therm
changes
presence
chosen h
pendix A

f
where

$$p' = \frac{1}{3}$$

are the ef
an appare
isotropic
added to i
the size of

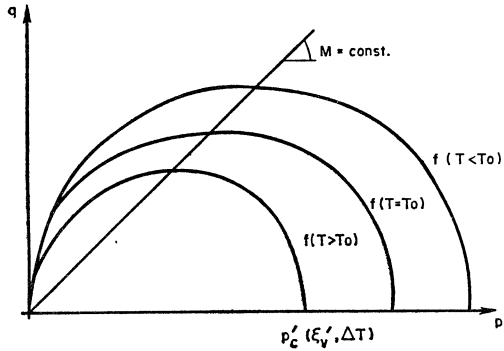


Fig. 1. Schematic of the yield surface sensitivity to temperature

The following assumptions concerning the behavior of the skeleton are made, based on the experimental evidence from drained tests, (Hueckel and Peano, 1987; Hueckel and Baldi, 1990).

The skeleton response to effective stress within the current yield surface is thermoelastic, and the response to changes of stress at the yield surface is thermoplastic. The yield surface in non-thermal conditions is a function of plastic volumetric strain, and may expand (strain hardening) or shrink (strain softening), depending on whether the rate of the volumetric strain is positive (compactive) or negative (dilative), respectively, according to the modified Cam-clay model (Roscoe and Burland, 1968). In thermal conditions the thermoelastic domain shrinks with an increasing temperature, and it expands, when cooling occurs, Fig. 1. The former effect is known as thermal softening, (Prager 1958). These changes may occur both without and in the presence of plastic strain. The yield surface, chosen here to be of elliptical shape (see Appendix A, Eq. (A-1) is thus

$$f = f(p', q, p'_c(\varepsilon_v^{tp}, \Delta T)) = 0 \quad (1)$$

where

$$p' = \frac{1}{3} (\sigma_1' + 2\sigma_3'); \quad q = (\sigma_1' - \sigma_3'), \quad (2)$$

are the effective stress invariants, while p'_c is an apparent maximum past preconsolidation isotropic stress. The adjective apparent is added to include the effect of temperature on the size of the yield surface. ε_v^{tp} is the thermo-

plastic volumetric strain and ΔT is the temperature difference with respect to the temperature at the initial state, $\Delta T = T - T_0$. The critical state parameter M is considered as constant. A discussion of this assumption follows in Section 5.

The laws of skeleton deformability adopted throughout this paper are those of coupled thermo-elasto-plasticity. The term coupled implies a dependence of isothermal behavior parameters (moduli) on temperature and of isobaric behavior parameter (expansion coefficients) on effective isotropic stress.

Thermoelastic volumetric strain, ε_v^{te} , generated during heating at constant effective isotropic stress p' , depends non-linearly on p' and on temperature. Drained experiments have shown (Hueckel and Peano, 1987; Hueckel and Baldi, 1990) that low porosity clays undergo thermal expansion at low effective isotropic stress, and thermal compression at higher effective stress (more than about 1 MPa). The latter effect, known as thermal consolidation, has also been reported by Passwell (1967), Campanella and Mitchell (1968), Demars and Charles (1982), Agar et al. (1986) and others. Elastic deviatoric strains are assumed as temperature independent and proportional to deviatoric stress. The expressions for thermoelastic strain are given in Appendix A.

At yielding, both elastic and plastic strains develop. Their rates follow the additivity principle. Thermoplastic strain rate was found in tests to be temperature rate dependent, both in terms of strain magnitude and strain mode, (see Hueckel and Baldi, 1990). The latter effect is important mainly during heating in drained conditions. In undrained conditions, stress rate induced deformation is substantially greater than thermal strain. In this paper the associated rule is assumed to describe thermoplastic strain rate. The relative equations are given in Appendix A, (Eqs. A-6 and A-7). As may be seen from these equations, the plastic deformability depends on the yield surface sensibility to temperature. This is defined through Eq. (A-2). The form of this equation has been chosen in a way to

keep separate the thermal and plastic strain dependence of the yield surface. As a consequence, although λ is constant, the ratio of logarithm of isotropic stress to volumetric strain is not, at high constant temperature. This is accepted in order to describe the yield surface changes with temperature in elastic states, when no plastic strain has yet developed. Thermoplastic loading and thermoplastic unloading ranges are defined through

$$f=0; \dot{f}=0; \Delta > 0 \quad (3)$$

and

$$f < 0, \text{ or } f=0; \dot{f} < 0 \quad (4)$$

respectively.

As it was mentioned previously, strain in the solid skeleton is caused in part by the direct action of heat and in part by heat induced pore water pressure rise. To evaluate the latter effect the thermal volume change of water in clay has to be determined.

Water in low porosity clays has different properties when compared to ordinary water. Due to small dimensions of pores, a large part of water is affected by the particle surface (Low, 1987; Derjaguin et al., 1987; Homola et al., 1989). Thermal volume change of clay water was found (Baldi et al., 1988) to depend on temperature, on a conventional interparticle spacing $2d$ in an idealized parallel particle system, and on effective stress. The volumetric strain of pore water per unit volume of soil is then:

$$\Delta \varepsilon^w = -\beta^w \Delta T + n C^w \Delta u, \quad \beta^w = \beta^w(T, \ln p', d) \quad (5)$$

where Δ denotes the difference referred to the state of heating onset. Equations (5) imply a coupling of thermal volume change of water to the interparticle distance of solid skeleton and effective stress in the solid skeleton. The explicit form of the expression for β^w is given in Appendix B.

The average interparticle half-spacing d , is obtained assuming that all thermal volume changes of the porous space in skeleton result from a change in distance of clay platelets arranged in a hypothetical parallel system as follows:

$$d = \frac{e_0 - (1 + e_0) \varepsilon_v - (1 - n) (C^* \Delta u - \alpha^* \Delta T)}{S_s G_s \gamma_w} \quad (6)$$

where γ_w is specific density of water, while G_s is specific gravity of clay solid particles, S_s is the specific surface area of mineral particles per unit weight of dry clay. For small strains, d may be considered as constant and the coupling is limited to the dependence of thermal expansion of pore water on the effective stress.

Saturation of clay and mass balance of water in undrained conditions, require that the volume change of water equals the volume change of pore space, the latter one expressed as the difference between total volume change of soil and that of solid mineral, i. e.

$$\Delta \varepsilon^w = \Delta \varepsilon_v + (1 - n) [C^* \Delta p' + \alpha^* \Delta T] \quad (7)$$

Furthermore, it is assumed that clay constituents, i. e. skeleton, adsorbed water and bulk (free) water interact mechanically in the transmission of total stress. The interaction is described by the rule of series connection of the two former elements, whereas the latter one is connected parallelly to them. This implies also the equality of effective stress and specific osmotic forces in the adsorbed water as well as the additivity of deformation of the skeleton and adsorbed water. The above may be considered as a generalization of the Terzaghi's effective stress principle. Although it is a conceptual model and does not refer to any particular microscopic mechanism, it does not contradict an interparticle contact interaction model (in which repulsive forces are usually small) nor a parallel face-to-face model (in which repulsive forces are equal to effective stress, see also—Sridharan and Jayadeva, 1982). Thus, under constant total stress conditions

$$\Delta p' = -\Delta u \quad (8)$$

EXPERIMENTS

Experiments were performed at ISMES, Bergamo, in a high stress, high temperature triaxial apparatus described elsewhere (Baldi et al., 1986). The experiments aimed at

detecting
thermon
saturate
are: unc
Boom cl
Boom c
plastic, a
water co
Pontida
quartz):
(30%) a

The e
specimen
constant
to a devi
which ge
applied c
situ stre
nuclear
1988).
attained,
constant
for 48
pressure
Heating
with inte
Pontida c
heating.
described
1989; 199
cooling v

To pre
the speci
of water
pansion c
porous st
check wa
water le.
pressure.
discussed
et al., 198

Figs. 2
on Pontid
developme
with resp
dation str
as temper
two heati
compressi

detecting the principal effects leading to thermomechanical failure. Tests on two saturated clays are described here. The clays are: undisturbed, anisotropic, overconsolidated Boom clay, and remolded Pontida silty clay. Boom clay from a 240 m depth is a highly plastic, about 20% smectitic material, with low water content (26%) and low permeability. Pontida is a kaolinitic/illitic silty clay (25% quartz) and has a little higher water content (30%) and low permeability.

The experiments consisted of heating of clay specimens in the undrained condition at a constant total stress. Specimens were subjected to a deviatoric stress in the undrained condition which generated some pore water pressure. The applied deviatoric stress corresponds to an in situ stress expected from emplacement of a nuclear waste container (Pellegrini et al., 1988). After the desired deviatoric stress was attained, clay specimens were left under constant load at a room temperature of 22°C for 48 hours. A modest creep and pore pressure build up was observed at this time. Heating was performed in temperature steps, with intermissions for stabilization. Boom and Pontida clays were subjected only to monotonic heating. In other tests on Pasquasia clay, described elsewhere (Hueckel and Pellegrini, 1989; 1991) cycles of undrained heating and cooling were also performed.

To prevent any change in water content in the specimen itself, small calibrated amounts of water, corresponding to the thermal expansion of the cell, and water in tubings and porous stones, were gradually released. Careful check was made to eliminate any influence of water leak on the measured pore water pressure. The details of the experiments are discussed elsewhere (Baldi et al., 1986, Baldi et al., 1988).

Figs. 2 and 3 show the results of the test on Pontida silty clay. Fig. 2 (a) presents the development of pore water pressure, normalized with respect to the constant isotropic consolidation stress as a function of the axial strain as temperature changes, curve (a). The first two heating steps after an initial undrained compression, produced a small axial extension

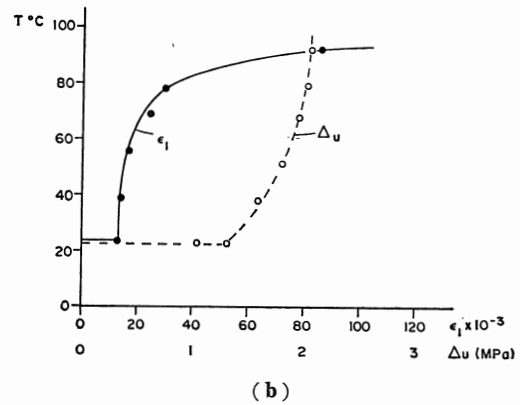
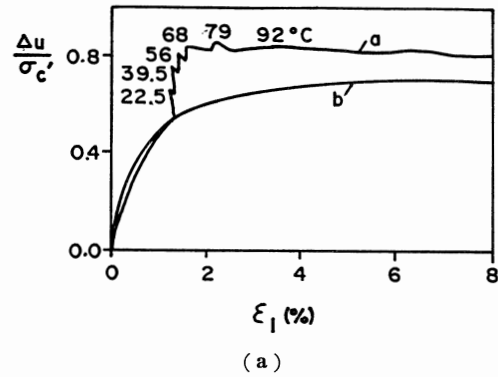


Fig. 2. Pontida silty clay. Undrained heating test: (a) water pressure vs. axial strain, (curve (a)—heating test; curve (b)—undrained compression test; (b) axial strain and water pressure vs. temperature

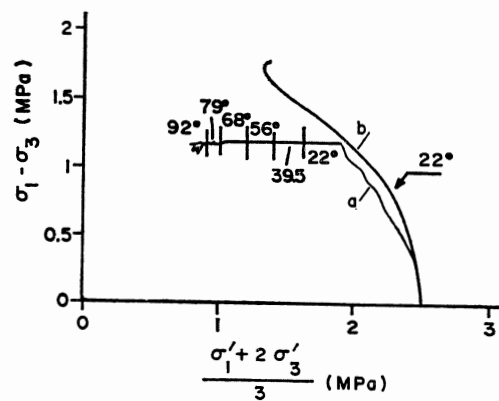
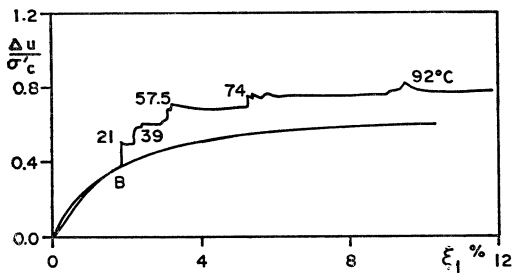


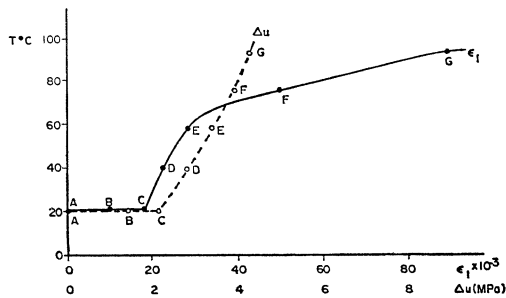
Fig. 3. Pontida silty clay. Undrained heating test: effective stress path

which was followed by contraction starting at the temperature about 38°C. Curve (b) gives the water pressure buildup as a function of strain in an usual undrained triaxial test for comparison. Thermally induced failure, without any visible shear band, occurred at about 90°C at axial strains around 3.5%, Fig. 2 (b). However, an increase of the rate of strain per centigrade was already observed at lower temperature and lower strain (79°C and 2.5%). Fig. 3 shows the effective stress path, (curve a) calculated according to the Terzaghi's effective stress principle from the pore water pressure readings. For comparison, the usual undrained triaxial test stress path obtained without heating is also shown, curve (b).

The results of undrained heating for Boom clay (Figs. 4(a), 4(b) and 5) are similar to those for Pontida clay, with a few exceptions. As opposed to Pontida clay, failure of Boom clay was associated with the formation of a shear band. No initial axial extension was observed. Also, the thermal water pressure



(a)



(b)

Fig. 4. Boom clay. Undrained heating test: pore water pressure vs. (a) vertical strain, (b) axial strain and water pressure vs. temperature

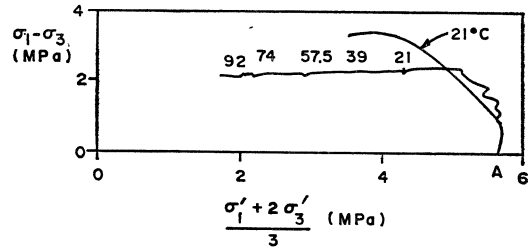


Fig. 5. Boom clay. Undrained heating test: effective stress path

buildup at failure was almost twice as high as in the experiment with Pontida clay, while the temperature at failure was nearly the same. Drained, constant stress, heating tests were also conducted on Pontida clay and are presented elsewhere (Hueckel and Baldi, 1990).

THERMOELASTOPLASTIC ANALYSIS OF UNDRAINED HEATING

We shall now discuss clay response to undrained heating in the light of the thermo-plastic model. In contrast to the usual idealization valid for isothermal undrained triaxial compression tests, during heating the volumetric strain of water and that of skeleton are not equal to zero. Rather, the volumetric strain of skeleton is such as to accommodate the resultant strain in water due to its thermal expansion and due to its compression caused by the growing water pressure. The tests were conducted at constant total stress, and thus Eq. (8) holds throughout.

The primary hypothesis employed in our considerations, is that due to the expansion during heating, a thermal pressurization of the pore water occurs and water gradually takes over the total isotropic stress from the skeleton. The water pressure increase implies a decrease of effective isotropic stress in the skeleton. At constant stress deviator this leads eventually to failure, as seen in Figs. 3 and 5. The question how this decrease in effective mean stress develops is the subject of this section.

The skeleton response to heating may either be initially elastic and then eventually plastic, or plastic from the very beginning,

what co
respecti
occur e
strain ha
explain
two hyp
6 and 7
part of
the yield
general,
to the o
are: (i)
to the th
thermal
ed by te
yield su
situation
water pr
is higher
the skele
of the v
loading)
then the
ing is g
degradati
effective
first case,
inside the
The strain
expansion
expansion
caused by

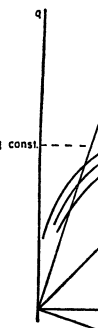


Fig. 6. St heating therm

what corresponds to inequalities (4) and (3) respectively. The onset of yielding may occur either at strain softening side or at strain hardening side of the yield surface. To explain these cases in detail let us consider two hypothetical situations presented in Figs. 6 and 7. In both cases the thermomechanical part of the effective stress path originates at the yield surface passing through point C. In general, there are two possible contributions to the observed effective stress change, which are: (i) elastic unloading of the skeleton due to the thermal water pressure buildup and (ii) thermal degradation of the skeleton represented by temperature dependent shrinking of the yield surface. Accordingly, at point C two situations are possible. If the rate of the water pressure buildup (and thus of unloading) is higher than that of thermal degradation of the skeleton, the process is elastic; if the rate of the water pressure buildup (and of unloading) is lower than the skeleton degradation, then the process is plastic and strain hardening is generated to slow down the thermal degradation of skeleton and to maintain the effective stress at the yield surface. In the first case, consider a generic point 1, which is inside the current yield surface $f_1=0$, Fig. 6. The strain rate in the skeleton is a volumetric expansion resulting from the elastic volumetric expansion due to a drop in effective stress, caused by the thermal water pressurization,

and of, usually much smaller, thermoelastic strain (thermal consolidation or expansion depending on the effective stress). Consequently, the projection of the strain rate vector on the axial direction, gives extension, $\dot{\epsilon}_1 < 0$.

The effective stress point may eventually meet the yield surface. This may occur either at the strain softening side of the yield surface ('to the left' from the critical state line), or at the strain hardening side ('to the right'). In the former case, the effective stress point is forced to return when it enters in contact with the continuously shrinking yield surface. Thus, in a typical point 3, Fig. 6, the strain rate is composed of a dilative plastic strain rate, normal to the yield surface and compressive elastic strain rate. The projection of both strain rate parts on the axial direction is compressive. Thus, at this stage the volume change of the pore space due to plastic dilatancy must be larger than the water expansion, to accommodate the elastic skeleton contraction.

The above described process may continue until the critical state line is met. In fact, to ensure the continuation of thermoplastic yielding the plastic multiplier λ defined through Eq. (A-8) must be positive, see Eq. (3). Therefore, since the plastic hardening modulus H_T is negative, when the effective stress point is at the strain softening side of the yield surface, the following inequality results:

$$\dot{p}'/\dot{T} > - \frac{\partial f}{\partial T} \bigg/ \frac{\partial f}{\partial p'} \quad (9)$$

From drained heating experiments at constant isotropic stress it has been concluded that $\partial f/\partial T$ is positive (Hueckel et al., 1987a). This implies that $\dot{p}' > 0$ for positive \dot{T} .

As the effective stress approaches the critical state, $\partial f/\partial p'$ tends to zero and thus \dot{p}' becomes unbounded to maintain inequality (9). This results in an unbounded drop in water pressure. If inequality (9) were not satisfied, the skeleton deformation could only be elastic. This however, is kinematically inadmissible. In fact, the elastic volumetric strain rate of pore space practically cannot be contractile, when the pore water expands, as it results

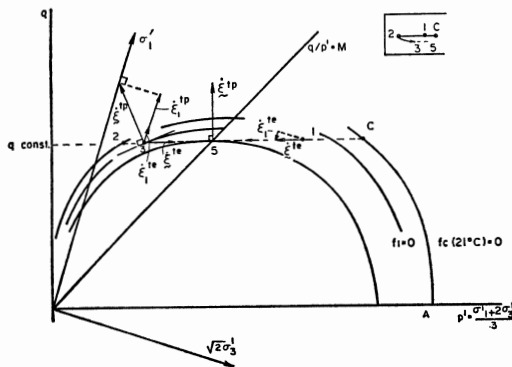


Fig. 6. Stress and strain rates during undrained heating. Scenario I: Elastic unloading and thermoplastic softening

A 6

est :

h as
hile
the
ests
are
(90).

OF

to
rmo-
ide-
ined
; the
leton
etric
odate
rml
used
ests
, and

our
nsion
of the
takes
leton.
rease
. At
tually
The
mean
tion.

may
tually
aning,

from Eq. (7). On the other hand, an expansive elastic volumetric strain implies $\dot{p} < 0$, what provokes an immediate yielding. At the intersection point of the stress path and the critical state line, also the deviatoric plastic strain rate tends to infinity. In fact, the yield surface normal has a zero isotropic component at this point, and by virtue of the expressions (A-8), and (A-9), the thermo-plastic multiplier λ tends to infinity for any \dot{T} . So does the axial plastic strain rate. This is considered here as failure.

Summing up, in this case, with the water pressure first growing up and then starting to drop at the strain softening side of the yield surface, failure due to heating is predicted at the critical state line. Failure implies unbounded axial strain and water pressure drop rates. However, compressive vertical strain would not show up before the pressure drop.

The other above mentioned situation at yielding is when the yield surface reaches the stress point at its hardening side. Yielding in this case starts at much lower value of water pressure. This is possible because the yield condition is a non-linear function of temperature, Baldi et al. 1988. This situation is analogous to, and will be considered below with, the case of the initial yielding at the point C.

To that end, consider a generic stress point 4 at yielding, Fig. 7. It should be noted that the effective stress rate vector at point 4, is

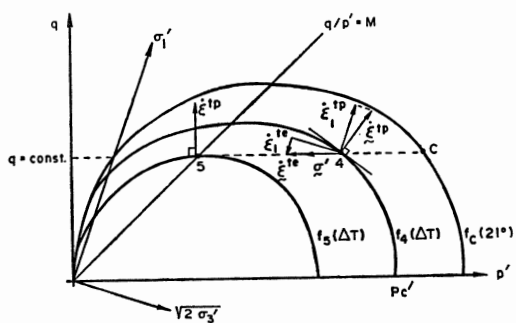


Fig. 7. Stress and strain rates during undrained heating. Scenario II: Thermoplastic hardening

directed toward the interior of the current yield surface, because of the thermal softening. This situation is admissible, if the numerator of the plastic multiplier λ , Eq. (A-8), is positive. This is the case when the effective stress rate at a given positive temperature rate satisfies inequality (9). As opposed to the situation at point 1 from Fig. 6, axial strain rate component may be contractile if the plastic strain rate is large enough. As the thermal shrinking of the yield surface continues, the contractile volumetric plastic strain rate component diminishes and eventually becomes zero. This again occurs at the point 5, of intersection of the stress path and the critical state line. Such point coincides with the top of the yield ellipse, which has the deviatoric semi-axis equal to the imposed deviatoric stress. Analogously to the previous case, at the critical state line the deviatoric and thus also axial plastic strain rate is unbounded and failure occurs, as may be seen from inequality (9). Any further heating leads to effective stress increments which are either kinematically or statically inadmissible.

Summing up, also in this case there is a possibility of failure due to heating at the critical state, but this is preceded by a monotonic water pressure growth and monotonic development of the plastic contractile strain in axial direction from early stages. At failure the axial strain rate tends to infinity, but the water pressure growth is finite.

Analyzing the two above cases the following conclusion may be reached. Thermomechanical failure may essentially be seen as a mechanical phenomenon, because in both possible cases it occurs when the effective stress reaches the critical state. Therefore, at the given stress path, the water pressure to failure is independent of temperature, but depends on the initial stress conditions and the internal friction angle. On the other hand, the temperature to failure is a function of elastic bulk modulus, thermal expansion coefficient of clay and that of clay water, thermal sensibility of the yield surface, as well as of the initial stress state, internal friction angle and overconsolidation ratio.

The above previous ex et al. (1986

NUMERIC ANALYSIS

In this S of the sim tests on B. Using the havior of volume cha and B), as may obtain pressure bu function of range. Thu

$$\Delta T(-n\beta^w + [nC^w$$

where p_0' re onset at C.

This equa temperature coefficients, of effective depends on

$$\Delta T = \frac{1}{2}(A_1 - [A_0 -$$

where

$$A_0 = \alpha^* +$$

$$B_0 = S_0$$

$$+ b_2$$

$$B_1 = S_1$$

$$+ b_5]$$

$$\bar{K} = \frac{K}{1 + e_0}$$

where $b_0 \dots$ Appendix B) the effective

The above theoretical conclusions agree with previous experimental observations by Agar et al. (1986) on oil sand.

NUMERICAL SIMULATIONS AND ANALYSIS

In this Section we shall discuss the results of the simulation of the undrained heating tests on Boom clay and Pontida silty clay. Using the constitutive equations for the behavior of solid skeleton and for thermal volume change of clay water (Appendices A and B), as well as the balance Eq. (7), we may obtain an expression for the water pressure buildup or effective stress drop as a function of temperature in the thermoelastic range. Thus writing explicitly Eq. (7) as

$$\Delta T(-n\beta^w + \alpha - (1-n)\alpha^*) = \frac{K}{1+e_0} \ln \frac{p'}{p_0} + [nC^w + (1-n)C^*] \Delta p' \quad (10)$$

where p_0' refers to the situation at the heating onset at C.

This equation can be solved explicitly for temperature only, because both expansion coefficients, β^w and α depend on the logarithm of effective stress while the water compression depends on the effective stress linearly. Thus

$$\Delta T = \frac{1}{2} (A_1 - nB_1)^{-1} \{ - (A_0 - nB_0) - [(A_0 - nB_0)^2 + 4\bar{K} (A_1 - B_1)]^{1/2} \} \quad (11)$$

where

$$A_0 = \alpha^* + \alpha_0 + \alpha_1 \ln \frac{p'}{p_0} \quad A_1 = \alpha_2 + \alpha_3 \ln \frac{p'}{p_0}$$

$$B_0 = S_s \gamma_w (1-n) \left[b_0 + b_1 \left(p_1 - \ln \frac{p'}{p_0} \right) + b_2 \left(p_1 - \ln \frac{p'}{p_0} \right)^2 \right] d$$

$$B_1 = S_s \gamma_w (1-n) \left[b_3 + b_4 \left(p_1 - \ln \frac{p'}{p_0} \right) + b_5 \left(p_1 - \ln \frac{p'}{p_0} \right)^2 \right] d,$$

$$\bar{K} = \frac{K}{1+e_0} \ln \frac{p'}{p_0} + [nC^w + (1-n)C^*] \Delta p'$$

where $b_0 \dots b_5$ are numerical constants (see Appendix B). An inverse of Eq. (10), giving the effective isotropic stress in terms of temper-

ature change, may be obtained numerically.

For the thermoplastic process an analogous rate equation may be obtained, relating temperature rate to pore pressure rate

$$-\dot{u} = \dot{p}' = \Omega \dot{T} \quad (12)$$

where

$$\Omega = \frac{-n \left(\beta^w + \frac{\partial \beta^w}{\partial T} \Delta T \right) + \alpha + \frac{\partial \alpha}{\partial T} \Delta T - \frac{1}{H_T} \left[\frac{\partial f}{\partial p'} \frac{\partial f}{\partial T} \right] - (1-n)\alpha^*}{-\left(-n \frac{\partial \beta^w}{\partial p'} + \frac{\partial \alpha}{\partial p'} \right) \Delta T + nC^w + \frac{1}{H_T} \left(\frac{\partial f}{\partial p'} \right)^2 + \frac{K}{1+e_0} \frac{1}{p'} + (1-n)C^*}$$

and where H_T is the thermoplastic hardening modulus defined in Appendix A by Eq. (A-9). Eq. (12) is valid if

$$f = 0, \dot{f} = 0 \text{ and } \Delta > 0 \quad (13)$$

Eq. (12) requires a numerical integration, since Ω depends both on T and p' .

Using Eqs. (11) and (12), a condition for thermoplastic yielding may be obtained. To that end we shall employ the unloading condition, $\dot{f} \leq 0$. Substituting in it the rate form of the expression for the effective stress in terms of temperature for the elastic range, Eq. (11), the unloading condition is reached for monotonically growing temperature, $\dot{T} > 0$. Then by exclusion, the following criterion for the onset of yielding is found:

$$\left(\frac{\partial f}{\partial p'} \Omega^e + \frac{\partial f}{\partial T} \right) > 0 \quad (14)$$

where

$$\Omega^e = \frac{-n \left(\beta^w + \frac{\partial \beta^w}{\partial T} \Delta T \right) + \left(\alpha + \frac{\partial \alpha}{\partial T} \Delta T \right) - (1-n)\alpha^*}{- \Delta T \left(-n \frac{\partial \beta^w}{\partial p'} + \frac{\partial \alpha}{\partial p'} \right) + (nC^w + (1-n)C^*) + \frac{K}{1+e_0} \frac{1}{p'}} \quad (15)$$

This condition is rate independent, because the stress path is fixed. However, this cannot be solved directly for ΔT or $\Delta p'$, because of an involved relationship between temperature and effective stress.

The total strain rate may now be obtained

for any \dot{T} for a given temperature and effective stress, by substituting into (A. 3-A. 7) the value of \dot{p}' from expression (12),

$$\dot{\epsilon}_v = (\Omega V^v + U^v) \dot{T} \quad (16a)$$

$$\dot{\epsilon}_q = (\Omega V^d + U^d) \dot{T} \quad (16b)$$

where

$$V^v = (p')^{-1} \frac{K}{1+e_0} - \frac{\partial \alpha}{\partial p'} \Delta T + \frac{1}{H_T} \left(\frac{\partial f}{\partial p'} \right)^2$$

$$V^d = \frac{1}{H_T} \frac{\partial f}{\partial p'} \frac{\partial f}{\partial q} \quad (17)$$

and

$$U^v = - \left(\alpha + \frac{\partial \alpha}{\partial T} \Delta T \right) + \frac{1}{H_T} \frac{\partial f}{\partial T} \frac{\partial f}{\partial p'} ;$$

$$U^d = \frac{1}{H_T} \frac{\partial f}{\partial T} \frac{\partial f}{\partial q} \quad (18)$$

Eq. (16) also require numerical integration. It is worthwhile to note that as the stress point approaches the critical state, the thermo-plastic hardening modulus H_T , (A-9), tends to zero. Deviatoric strain rate Eq. (16b) also tends to an infinite value at the critical state,

since U^d becomes unbounded. This is understood as failure.

The numerical simulations were performed using a computer program based on time integration, using finite difference technique for an arbitrary stress path. The results of the simulations of the experiments discussed in Section 3 (Figs. 2-5), are presented in Figs. 8 and 9. From these experiments it may be observed, that the first case of failure discussed in the previous section, did not develop in any of the tests. In fact, the axial strains were contractile all the time in Boom clay. Thus in Boom clay the process appears to be entirely plastic. In Pontida clay, axial strains initially were expansive, but became contractile well before the intersection of the stress path with the critical line. Moreover, the water pressure has not fallen catastrophically at failure in any of the tests.

Simulations of thermomechanical failure test on Boom clay were performed for two different values of the coefficient $M=0.87$ and 1.045. The former value is an average for all Boom specimens tested in this program, the latter is that reached in the test. Mechanical and thermomechanical constants for Boom clay were obtained previously from drained tests, Baldi et al., (1987), and are given in Appendix C. From Fig. 8(a) it may be seen, that the predicted water pressure is underestimated in the first part of the heating process. This tendency reverses closer to failure. Axial strains are also underestimated for lower temperatures and overestimated for higher. Moreover, $M=1.045$ implies an elastic response up to 37°C, Fig. 8(b).

The high value of M reached in the test, $M=1.045$, may have been caused by heating. The increase of the strength with temperature could be explained by the thermal disruption of the special water structure in fine pores (Derjaguin et al., 1987). Clays containing a well developed adsorbed water seem to have lower strength than these of low activity (Olson, 1974; Homola et al., 1989). Thus, heat could increase strength of Boom clay and should have a little effect on Pontida clay, which is a kaolinitic/illitic clay. In fact, Pontida

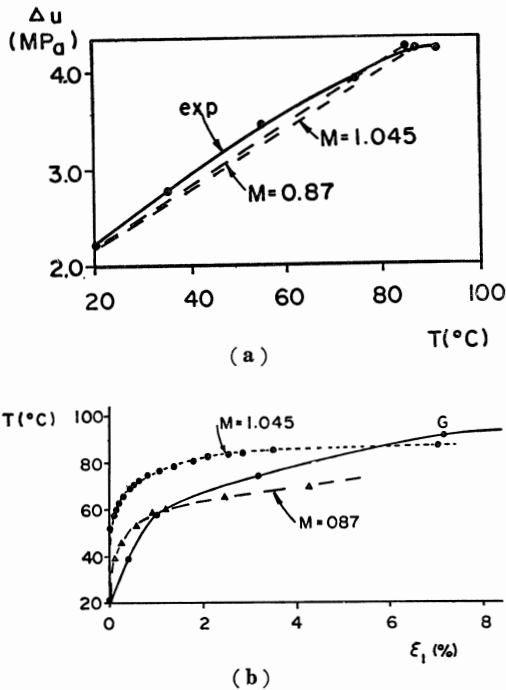


Fig. 8. Simulation of undrained thermomechanical failure in Boom clay (a) water pressure (b) axial strain

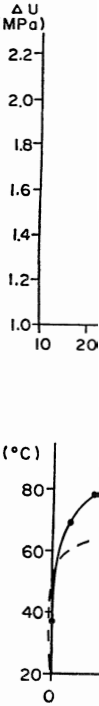


Fig. 9. Simulation of failure pressure

clay failed i
is below th
question re

The resu
Pontida silt;
(b). Num
in Append
given temp
and then an
was obtaine
close to fail
is require
than in th
Fig. 9(b).

DISCUSSIO

The above
pressure bu
an inaccura

under-

formed
1 time
hnique
sults of
scussed
ited in
may be
scussed
in any
s were
Thus in
entirely
initially
well be-
h with
ressure
lure in

ure test
r two
.87 and
e for all
m, the
hanical
om clay
d tests,
ppendix
that the
ated in
. This
Axial
lower
higher.
esponse

he test,
heating.
perature
ruption
e pores
aining a
to have
activity
Thus,
om clay
ida clay,
Pontida

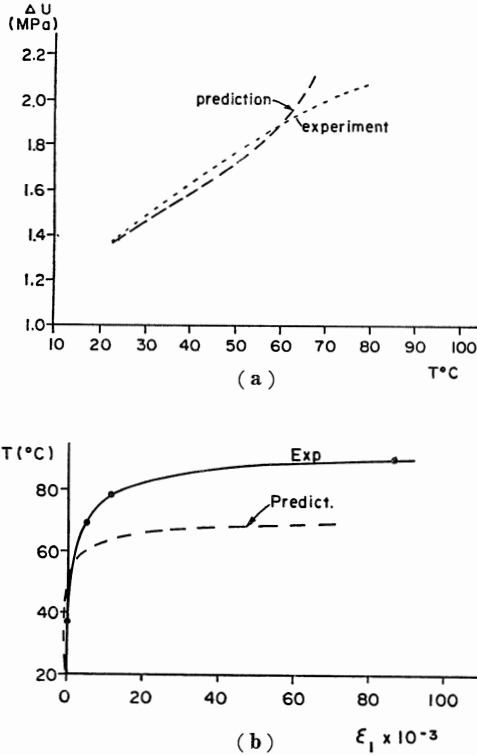


Fig. 9. Simulation of undrained thermomechanical failure in Pontida silty clay. (a) water pressure (b) axial strain

clay failed in the thermal test at $M=1.30$ which is below the mean value for this clay. This question requires further investigations.

The results obtained in the simulation of Pontida silty clay are shown in Fig. 9(a) and (b). Numerical values of constants are listed in Appendix C. In this simulation, for a given temperature an initial underestimation, and then an overestimation of pore pressure was obtained, the latter becoming significant close to failure. As a result, a lower temperature is required to cause failure in the simulation than in the experiment, as readily seen in Fig. 9(b).

DISCUSSION

The above indicated overestimation or pore pressure buildup at failure may result from an inaccurate prediction of the plastic volu-

metric strain. Apparently, in the vicinity of the critical state, the actual plastic strain rate becomes dilative rather than compressive, as would result from the associative flow rule in the modified Cam clay model. Note that from the mechanical point of view, the response to heating may be seen as a volumetric straining of the skeleton, to accommodate the pore water expansion. Thus in the presence of large plastic dilatancy, less elastic dilation is induced resulting in a smaller effective stress drop than predicted. Similar non-linearities in the response of pore pressure to temperature were obtained experimentally in triaxial, constant stress heating tests on oil sands by Agar et al., (1986). The non-linear pore pressure development is even more pronounced in another clay, viz. Pasquasia clay discussed elsewhere (Hueckel and Pellegrini, 1989). Upon heating above 70°C a water pressure drop of about 25% of the total value was observed in this clay. Such a response cannot be interpreted in the framework of the modified Cam clay model with associated flow rule. An alternative thermomechanical model for clay should be developed allowing for dilative hardening, like the model proposed by Nova (1982). However, there is a lack of experimental evidence at this moment, whether the observed non-associativity is a feature of clay skeleton behavior due to mechanical loading or it is a thermal effect.

A predictable dependence of the temperature

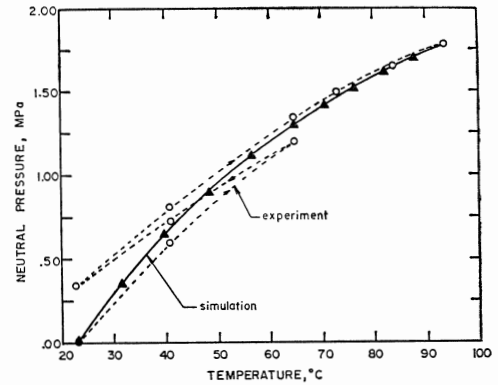


Fig. 10. Pontida silty clay. Isotropic undrained heating

to failure on the deviatoric stress has not yet been studied experimentally. Heating tests in undrained conditions at constant isotropic stress were performed on Pontida silty clay, see Fig. 10. However, they never led to failure, in the range of tested temperatures, $T \leq 95^\circ\text{C}$. This confirms also the hypothesis that thermomechanical failure is not a purely thermal or thermochemical process, but rather it depends on the mechanical conditions of the material. In the simulation of this process the response was always elastic. The experiment has shown a small residual value of the water pressure upon heating and cooling. It is interesting to note that the value of the water pressure at 95°C is almost twice as high as in the presence of the deviator in the test in Fig. 2. This again supports the hypothesis that close to failure a substantial plastic dilatancy develops which accomodates a large part of thermal water expansion.

CONCLUSIONS

Thermomechanical failure of saturated clay observed in undrained conditions under constant total stress was interpreted and simulated numerically using a thermoelastoplastic model for saturated clays. The experiments show the development of plastic compressive axial strain due to heating. Failure is associated with a pore pressure buildup and unconfined increase of the strain and of its rate. The model employed to stimulate this behavior is a combination of Cam Clay and a thermoplasticity theory for the skeleton, with a non-linear thermoelasticity for clay pore water. According to this model, thermomechanical failure occurs due to the pore water pressure buildup, causing the effective stress decrease up to the critical state. The stress decrease is associated with thermoplastic strain. This mechanism was well predicted by simulations at stages prior to failure state. Modeling of thermoplastic strain is essential for the simulation. Material constants of the model were evaluated on the basis of drained tests described elsewhere.

The model seems to be consistent with the

findings from the undrained heating experiments. This allows us to attempt the following conclusions. According to the present model the temperature to failure is essentially not a thermal property of clay material itself but depends on mechanical and thermomechanical clay properties, as well as on the initial effective stress and the overconsolidation. Similar conclusions were reached by Agar et al. (1986). On the other hand, the water pressure to failure according to the model is independent of temperature and is a function of the initial effective stress and the critical state parameter (or internal friction angle). The latter one appears to be little or not sensible to temperature at all. A correct prediction of the water pressure buildup is necessary to evaluate the possibility of hydraulic fracturation of clay (Bjerrum, 1972).

At effective stress states closer to failure, a substantial plastic dilatancy at strain hardening has presumably occurred, causing a reduction of the rate of water pressure buildup. In one of the tested clays, also the value of the water pressure dropped. However, it should be further investigated whether such a dilatancy actually takes place and if so, whether it is a purely mechanical or a thermomechanical effect.

Thermomechanical failure in saturated clay is yet to be verified experimentally in situ. It may be a cause of non-linearities of thermal conductivity, by a sort of hydraulic fracturation observed close to heat source in some field tests, (Tassoni, 1980). In the numerical simulations of boundary value problems (Hueckel and Peano, 1987) thermal yielding was predicted around the heat source, but with no global collapse.

ACKNOWLEDGMENTS

The authors are indebted to Mr. Giuseppe Angeloni, a technician of ISMES who performed the tests with a great commitment.

Part of the work at Duke University was supported by a grant from ISMES, Bergamo Italy. The work at ISMES has been carried out as a part of research program supported by ENEL (National Board of Electricity

Italy), ENEA (Energy of Italy European Comm

APPENDIX A

The expression dependent, yield

$$f = \left(\frac{2p'}{p_c'(\epsilon_v^{pt}, \Delta T)} \right)$$

The apparent pre is represented by ellipse (A-1), p_c'

$$p_c' = 2 \left(\bar{a} \exp \left\{ \frac{\dots}{\lambda} \right\} + a_1 \Delta T + a_2 \text{sig} \right)$$

where \bar{a} is a dimension are the initial void conventionally to th respectively; a_1 an thermal sensibility of the tested clays a_1 a temperature dependent us. The thermoelas

$$\epsilon_v^{te} = \frac{K}{1 + e_0}$$

$$\epsilon_q^{te} = \frac{1}{3G} (q$$

where K is the consta us and G is the cons e_0 are values of p' an is a variable o expansion of clay an clay solid mineral, α^* skeleton, $\bar{\alpha}$. The latte s physio-chemical coe and Mitchell, 1968, defi

$$\bar{\alpha} = \alpha - \alpha^*$$

assumed here to have

$$\bar{\alpha} = \alpha_0 + (\alpha_1 + \alpha_3 \Delta T)$$

$$\Delta T = T - T_0;$$

where $\alpha_0 \dots \alpha_3$ are coeffic

experi-
llowing
t model
y not a
self but
chanical
initial
lidation.
Agar et
e water
model is
function
critical
angle).
or not
correct
ildup is
ility of
1, 1972).
ailure, a
ardening
eduction
In one
of the
it should
dilatancy
r it is a
cal effect.
ated clay
situ. It
f thermal
cturation
ome field
ical simu-
(Hueckel
ling was
t with no

Giuseppe
who per-
itment.
ersity was
Bergamo,
en carried
supported
ctricity of

Italy), ENEA (National Board for Alternative Energy of Italy) and by the Comission of European Communities.

APPENDIX A

The expression for the adopted temperature dependent, yield surface is

$$f = \left(\frac{2p'}{p_c'(\epsilon_v^{tp}, \Delta T)} \right)^2 + \frac{4q^2}{[Mp_c'(\epsilon_v^{tp}, \Delta T)]^2} - 1 = 0 \tag{A-1}$$

The apparent preconolidation isotropic stress is represented by an axis of the yield surface ellipse (A-1), $p_c'(\epsilon_v^{tp}, \Delta T)$ given by

$$p_c' = 2 \left(\bar{a} \exp \left\{ \frac{1}{\lambda - K_T} [e_1 + (1 + e_0)\epsilon_v^{tp}] \right\} + a_1 \Delta T + a_2 \text{sign}(\Delta T) \Delta T^2 \right); \tag{A-2}$$

where \bar{a} is a dimensional coefficient, e_0 and e_1 are the initial void ratio and that referred conventionally to the state at $p' = 10 \text{ KN/m}^2$, respectively; a_1 and a_2 are coefficients of thermal sensibility of the yield surface. For the tested clays a_1 and a_2 negative, K_T is a temperature dependent logarithmic bulk modulus. The thermoelastic constitutive law is

$$\begin{aligned} \epsilon_v^{te} &= \frac{K}{1 + e_0} \ln \frac{p'}{p_0'} - \alpha \Delta T; \\ \epsilon_q^{te} &= \frac{1}{3G} (q - q_0) \end{aligned} \tag{A-3}$$

where K is the constant isothermal bulk modulus and G is the constant shear modulus. p_0' , q_0 are values of p' and q at the initial state, α is a variable coefficient of thermal expansion of clay and includes that of the clay solid mineral, α^* , and that of porous skeleton, $\bar{\alpha}$. The latter coefficient referred to as physio-chemical coefficient by Campanella and Mitchell, 1968, defined as

$$\bar{\alpha} = \alpha - \alpha^* \tag{A-4a}$$

is assumed here to have the following form

$$\begin{aligned} \bar{\alpha} &= \alpha_0 + (\alpha_1 + \alpha_3 \Delta T) \ln \frac{p'}{p_0'} + \alpha_2 \Delta T; \\ \Delta T &= T - T_0; \end{aligned} \tag{A-4b}$$

where $\alpha_0 \dots \alpha_3$ are coefficients of thermoplastic

sensitivity of the clay skeleton.

Thus the bulk modulus K_T reads

$$K_T = \frac{K}{1 + e_0} + (\alpha_1 + \alpha_3 \Delta T) \Delta T \tag{A-5}$$

The thermoplastic flow rules are the following

$$\dot{\epsilon}_v = \dot{\epsilon}_v^{te} + \dot{\epsilon}_v^{tp}; \quad \dot{\epsilon}_q = \dot{\epsilon}_q^{te} + \dot{\epsilon}_q^{tp} \tag{A-6}$$

$$\dot{\epsilon}_v^{tp} = \Lambda \frac{\partial f}{\partial p'}; \quad \dot{\epsilon}_q^{tp} = \Lambda \frac{\partial f}{\partial q} \tag{A-7}$$

where a dot denotes rate. Λ is thermo-plastic multiplier

$$\Lambda = \frac{1}{H_T} \left[\frac{\partial f}{\partial p'} \dot{p}' + \frac{\partial f}{\partial q} \dot{q} + \frac{\partial f}{\partial T} \dot{T} \right] \tag{A-8}$$

$$H_T = - (1 + e_0) \frac{\partial f}{\partial p_c'} \frac{\partial p_c'}{\partial \epsilon_v^{tp}} \frac{\partial f}{\partial p'} \tag{A-9}$$

where H_T is the plastic hardening modulus.

APPENDIX B

Thermal expansion of clay water

Effective specific thermal volumetric expansion of water in low porosity clays is calculated as an integrated change in volume due to heating per unit pore space of adsorbed water subjected to holding forces of adsorption to mineral surface. The forces are assumed to be exponentially distributed across the pore half space idealized as infinitely long flat box. Usual dependence of water expansion on pressure and temperature is adopted. The effective coefficient of thermal expansion in low porosity clay thus reads (Baldi et al., 1988)

$$\begin{aligned} \beta^w &= S_s \gamma_w (1 - n) \bar{a} \left\{ b_0 + b_1 \left(p_1 - \ln \frac{p'}{p_0'} \right) \right. \\ &+ b_2 \left(p_1 - \ln \frac{p'}{p_0'} \right)^2 + \left[b_3 + b_4 \left(p_1 - \ln \frac{p'}{p_0'} \right) \right. \\ &\left. \left. + b_5 \left(p_1 - \ln \frac{p'}{p_0'} \right)^2 \right] T \right\} \end{aligned} \tag{B-1}$$

where the coefficients b_i are combinations of constants from the above quoted water expansion formula :

$$\begin{aligned} b_0 &= \bar{\alpha}_0 + (p_1 + \bar{m}) \bar{\alpha}_1 + (p_1 + \bar{m})^2 \bar{\alpha}_2; \\ b_1 &= -\frac{1}{2} [\bar{\alpha}_1 + \bar{\alpha}_2 (p_1 + \bar{m})]; \quad b_2 = \frac{1}{3} \bar{\alpha}_2; \end{aligned}$$

$$b_3 = \bar{\beta}_1(p_1 + \bar{m}) + \bar{\beta}_2(p_1 + \bar{m})^2 \quad (\text{B-2})$$

$$b_4 = -\frac{1}{2}[\bar{\beta}_1 + \bar{\beta}_2(p_1 + \bar{m})] \quad b_5 = \frac{1}{3}\bar{\beta}_2$$

$$\begin{aligned} \bar{\alpha}_0 &= 4.505 \times 10^{-4} (\text{°C})^{-1} & \bar{\beta}_1 &= -1.2 \times 10^{-6} (\text{°C})^{-2} \\ \bar{\alpha}_1 &= 9.156 \times 10^{-5} (\text{°C})^{-1} & \bar{\beta}_2 &= -5.766 \times 10^{-8} (\text{°C})^{-2} \\ \bar{\alpha}_2 &= 6.381 \times 10^{-6} (\text{°C})^{-1} & \bar{m} &= 1.8977 \end{aligned}$$

$$\text{while } p_1 = \ln \frac{p_{\max}}{\sigma_0}$$

is the logarithm of the ratio of a fictitious maximum-stress at the mineral water contact assumed as 2GPa, to a reference stress σ_0 taken as 100 MPa.

APPENDIX C

Constitutive constants and parameters for the numerical simulations

Boom Clay

$$\begin{aligned} w(\text{natural}) &= 19\% \\ e_0 &= 0.589 \\ G &= 100 \text{ MPa} \\ \lambda_0 &= 0.031 \\ M &= 0.87; 1.045 \\ \lambda &= 0.129 \\ C^* &= 2 \times 10^{-5} \text{ MPa}^{-1} \\ C^w &= 4 \times 610^{-4} \text{ MPa}^{-2} \\ T_0 &= 20^\circ\text{C} \\ \alpha_0 &= 4.5 \times 10^{-5} (\text{°C})^{-1} \\ \alpha_2 &= 2.5 \times 10^{-8} (\text{°C})^{-2} \\ \alpha_3 &= -3.18 \times 10^{-7} (\text{°C})^{-2} \\ \alpha^* &= 1 \times 10^{-5} (\text{°C})^{-1} \\ \alpha_1 &= -9 \times 10^{-8} \text{ MPa} (\text{°C})^{-1} \\ \alpha_2 &= -4.7 \times 10^{-5} \text{ MPa} (\text{°C})^{-2} \end{aligned}$$

Pontida Silty Clay

$$\begin{aligned} w(\text{natural}) &= 28\% \\ &= 0.805 \\ &= 48 \text{ MPa} \\ &= 0.0164 \\ &= 1.429 \\ &= 0.103 \\ &= 2 \times 10^{-5} \text{ MPa}^{-1} \\ &= 4.6 \times 10^{-4} \text{ MPa}^{-1} \\ &= 21^\circ\text{C} \\ &= 8.221 \times 10^{-5} (\text{°C})^{-1} \\ &= 6.00 \times 10^{-7} (\text{°C})^{-2} \\ &= 1.311 \times 10^{-7} (\text{°C})^{-2} \end{aligned}$$

$$\begin{aligned} &= 1 \times 10^{-5} (\text{°C})^{-1} \\ &= -10.56 \times 10^{-8} \text{ MPa} (\text{°C})^{-1} \\ &= -2.85 \times 10^{-4} \text{ MPa} (\text{°C})^{-2} \end{aligned}$$

REFERENCES

- 1) Agar, J. G., Morgenstern, N. R. and Scott, J. D. (1986): "Thermal expansion and pore pressure generation in oil sands," *Can. Geotech. July 23*, pp. 327-333.
- 2) Baldi, G., Borsetto, M., Hueckel, T. and Tassoni, E. (1986): Thermally induced strain and pore pressure in clays, *Proc. Int. Symp. on Environmental Geotechnology*, Allentown, Pennsylvania, H. Y. Fang, Envo Publ. Co. Bethlehem Pa.
- 3) Baldi, G., Hueckel, T. and Pellegrini, R. (1988): "Thermal volume changes of mineral-water system in low porosity clay soils," *Can. Geotech. J.*, v. 25, n. 4, pp. 807-825.
- 4) Bjerrum, L. et al. (1975): "Hydraulic fracturing in field permeability testing," *Géotechnique*, 22, 2, pp. 319-332.
- 5) Campanella, R. G. and Mitchell, J. K. (1968): "Influence of temperature variations on soil behavior," *ASCE Jnl. of Soil Mechanics and Foundation Division*, 94 (SM3): pp. 709-734.
- 6) Claesson, P. M., Kjellander, R., Stenius, P. and Christenson, H. K. (1986): "Direct measurement of temperature dependent interactions between non-ionic surfactant layers," *J. Chem. Soc. Faraday Trans., I*, 82, pp. 2735-2746.
- 7) Davies, T. G. and Banerjee, P. L. (1980): "Constitutive relationships for ocean sediments subjected to stress and temperature gradients," *AERE Harwell Rep. No. HL 80/2604 (C22)*, Aug. 1980.
- 8) Demars, K. R. and Charles, R. (1982): "Soil volume changes induced by temperature cycling," *Canadian Geotechnical Jnl.*, 19, 188-194.
- 9) Derjaguin, B. V., Churaev, N. V. and Muller, V. M. (1987): *Surface Forces*, Consultants Bureau, New York 1987.
- 10) Homola, A. M., Israelachvili, J. N., Gee, M. L. and Mc. Guiggan, P. M. (1989): "Measurements of and relation between the adhesion and friction of two surfaces separated by molecularly thin liquid films," *J. Tribology*, 111, p. 675.
- 11) Hueckel, T. and Borsetto, M. (1990): Thermo-plasticity of Saturated Soils and Shales: Constitutive Equations, *J. of Geotechn. Eng.*, 116, pp. 1705-1777.
- 12) Hueckel, T. and Baldi, G. (1990): Thermo-

plastic Beha
perimental C
13) Hueckel, T.
(1987a): "M
plastic-hydra
nuclear waste
in Transient
Lewis, E. Hi
fler, (editors
pp. 213-235.
14) Hueckel, T.,
(1987b): "A
coupling in
disposal," *Pr
Laws for Eng
Application, T
15) Hueckel, T.
geotechnical a
lation in con
Geotechnics, 3
16) Hueckel, T. ar
ing of therma
Numerical Me
Pietruszczak, an
90.
17) Low, P. F. (1
the swelling pr
pp. 18-25.
18) Nova, R. (198
soil under mon
13, *Soil Mecha
ed. G. N. Pan
Wiley.
19) Olson, R. E. (
kaolinite, illite
Geotech. Engin.
1215-1229.
20) Passwell, R. E. i
clay consolidatio
21) Pellegrini, R., i
Tassoni, E. (1
thermo-hydro-m
the safety assess
tories," in "E
radioactive waste
engineering desi
Proc. of Work
Canada.
22) Prager, W. (1958
formation," *Bol.*
8, 61/3, pp. 176-1
23) Pusch, R. (1987):
traction, a prima**

- plastic Behavior of Saturated Clays: An Experimental Constitutive Study, 116, pp. 1778-1796.
- 13) Hueckel, T., Borsetto, M. and Peano, A. (1987a): "Modelling of coupled thermo-elasto-plastic-hydraulic response of clays subjected to nuclear waste heat," in 'Numerical Methods in Transient and Coupled Problems', R. W. Lewis, E. Hinton, P. Bettess and B. A. Schrefler, (editors), J. Wiley, Chichester, U.K. pp. 213-235.
- 14) Hueckel, T., Borsetto, M. and Peano, A. (1987b): "A study of thermo-plastic hydraulic coupling in clays applied to nuclear waste disposal," Proc. 2nd Int. Conf. Constitutive Laws for Engineering Materials; Theory and Application, Tucson, Arizona, v. 1, pp. 311-318.
- 15) Hueckel, T. and Peano, A. (1987): "Some geotechnical aspects of radioactive waste isolation in continental clays," Computers and Geotechnics, 3, pp. 157-182.
- 16) Hueckel, T. and Pellegrini, R. (1989): "Modeling of thermal failure of saturated clays," in Numerical Models in Geomechanics, eds. S. Pietruszczak, and G. N. Pande, Elsevier, pp. 81-90.
- 17) Low, P. F. (1987): "Structural component of the swelling pressure of clays," Langmuir, 3, pp. 18-25.
- 18) Nova, R. (1982): "A constitutive model for soil under monotonic and cyclic loadings," Ch. 13, Soil Mechanics, Transient and cyclic loads, ed. G. N. Pande and O. C. Zienkiewicz, J. Wiley.
- 19) Olson, R. E. (1974): "Shearing strengths of kaolinite, illite and montmorillonite," Jnl. Geotech. Engin. Div., ASCE, 100, GT11, pp. 1215-1229.
- 20) Passwell, R. E. (1967): "Temperature effects on clay consolidation," ASCE, SM 3, pp. 9-21.
- 21) Pellegrini, R., Borsetto, M., Peano, A. and Tassoni, E. (1988): "Factors affecting the thermo-hydro-mechanical response of clay in the safety assessment of nuclear waste repositories," in "Excavation responses in deep radioactive waste repositories-implications for engineering design and safety performance," Proc. of Workshop, Winnipeg, Manitoba, Canada.
- 22) Prager, W. (1958): "Non isothermal plastic deformation," Bol. Koninke Nederl. Acad. Wet. 8, 61/3, pp. 176-182.
- 23) Pusch, R. (1987): "Permanent crystal lattice contraction, a primary mechanism in thermally induced alteration of Na bentonite," in Scientific Basis for Nuclear Waste Management X, ed: J. K. Bates and W. B. Seefeldt, MRS v. 84, pp. 791-802, Pittsburgh.
- 24) Pusch, R. and Guven, N. (1988): Electron microscopic examination of hydrothermally treated bentonite clay, Proc. of Workshop on Artificial clay Barriers for high level radioactive waste repositories, Lund, Sweden pp. 35-45.
- 25) Roscoe, K. and Burland, J. (1968): "On generalized stress strain behaviour of wet clay," in: Engineering Plasticity, J. Hayman and F. A. A. Leckie (eds) Cambridge Un. Press.
- 26) Schofield, A. N. and Wroth, C. P. (1968): *Critical State Soil Mechanics*, McGraw Hill, London.
- 27) Sridharan, A. and Jayadeva, P. (1982): Double Layer Theory and Compressibility of Clays, *Geotechnique* 32, 2, pp. 133-142.
- 28) Tassoni, E. (1980): An experiment on the heat transmission in a clay rock," Proc. of Workshop, "The Use of Argillaceous Materials for the Isolation of Radioactive Waste," pp. 23-45, OECD Paris.

List of Symbols

$f=0$ —yield surface

$p' = \frac{1}{3}(\sigma_1' + 2\sigma_3')$ —isotropic stress

$q = \sigma_1' - \sigma_3'$ —deviatoric stress

p_c' —apparent maximum isotropic past precompression stress

$\epsilon_v = \epsilon_1 + 2\epsilon_3$ —total volumetric strain, ϵ_1 and ϵ_2 —axial and lateral strain components

ϵ_v^{tp} —thermoplastic volumetric strain

ϵ_v^{te} —thermoelastic volumetric strain

$\epsilon_q = \frac{2}{3}(\epsilon_1 - \epsilon_3)$ —deviatoric total strain

$T, \Delta T = T - T_0$ —temperature in °C

T_0 —reference (laboratory) temperature

ϵ^w —volumetric strain in water or specific volume change in water (positive in compression)

β^w —specific volume change of water per °C at $\Delta T = T - T_0$,

n —porosity

C^w —water compressibility coefficient

Δu —water pressure excess

d —average interplatelet distance between parallel arranged clay plates

e_0 =initial void ratio	γ_w =specific density of water
C^* =compressibility of clay solid mineral	K_T, K_0 =thermal and isothermal logarithmic compressibility bulk modulus of clay
α^* =thermal expansion coefficient of clay solid mineral	α =global thermal expansion coefficient (variable) of clay, see (A-4a and A-4b)
G_s =specific gravity of clay solid particles	λ =thermoplastic bulk modulus
S_s =specific surface area of skeleton particles	